Dipole bands in nucleus ^{139}Pm*

ZHANG Ning-Tao(张宁涛)[1,2] ZHANG Yu-Hu(张玉虎)[1,2;1)] ZHOU Xiao-Hong(周小红)[1]
LIU Min-Liang(柳敏良)[1] ZHENG Yong(郑勇)[1] GUO Ying-Xiang(郭应祥)[1] CHEN Liang(陈亮)[1,2]
WANG Shi-Tao(王世陶)[1,2] ZHANG Xin(张昕)[1,2] ZHU Li-Hua(竺礼华)[3] WU Xiao-Guang(吴晓光)[3]

[1] Institute of Modern Physics, Chinese Academy of Sciences, Lanzhou 730000, China
[2] Graduate University of Chinese Academy of Sciences, Beijing 100049, China
[3] China Institute of Atomic Energy, Beijing 102413, China

Abstract High-spin states in nucleus ^{139}Pm have been studied using the reaction ^{116}Cd(^{27}Al, 4n)^{139}Pm. Two dipole cascades have been found. Spin and parity assignments were based on the Directional Correlation of Oriented Nuclei (DCO) ratios and systematic behavior in neighboring odd-proton nuclei. The level structures of ^{139}Pm are compared with those of the $N=78$ isotone ^{141}Eu in which two dipole bands have been confirmed as magnetic rotational bands. The close similarity between them suggests that the dipole bands in ^{139}Pm may be magnetic rotational bands.

Key words magnetic rotation, soft nuclei, driving force, oblate shape

PACS 21.60.Ev, 23.20.Lv, 27.60.+j

1 Introduction

Magnetic rotation (MR) phenomenon, observed more than a decade ago, has aroused great interest from the nuclear structure community. These regular sequences of M1 transitions show rotation-like bands in almost spherical nuclei [1, 2]. Contrary to normaldeformed (ND) and superdeformed (SD) rotational bands, the dipole MR bands exhibit strong intraband magnetic dipole transitions whereas the crossover E2 transitions are either weak or almost absent. This rotational behavior has been difficult to understand in terms of the rotational model because of the rather small deformation. Frauendorf [3] proposed an explanation for the MR bands in terms of a shears mechanism and interpreted these sequences using the tilted-axis-cranking (TAC) model. A coupling of high-j proton particles (holes) in low (high) Ω orbital and high-j neutron holes (particles) in high (low) Ω orbital leads to a nearly perpendicular coupling of angular momentum vectors. The neutron and proton angular momentum vectors represent the two blades of the shears which close with increasing angular momentum and energy. Consequently, the total angular momentum axis does not coincide with one of the principal axes of the nucleus. The perpendicular coupling of the particle and hole orbitals, each with high spin j, results in a large transverse component of the magnetic moment vector and creates the enhanced M1 transitions between the shears states. Experimental proofs for the shears mechanism are the decreasing B(M1) values with increasing spin and the termination of the bands when the shears are closed. These have been confirmed in many MR bands [4–6].

In the mass A=130–140 region, magnetic rotations are expected where high-j nucleons are available and the deformation is small. For the $N\approx 78$ region MR bands are expected and have been found, e.g. in ^{136}Ce [7], ^{137}Pr [8], ^{139}Sm [9], ^{141}Eu [10]. It is, therefore, of interest to investigate whether some MR bands develop in the Pm nuclei.

The nucleus ^{139}Pm had been studied earlier by van Klinken et al. [11] using the decay of ^{141}Eu and by Xu et al. [12], using the ^{116}Cd(^{27}Al, 4n)^{139}Pm reaction. In the present work, we focus upon a partial level scheme of ^{139}Pm nuclide and two ΔI=1 bands have been identified as potential candidates of MR bands.

Received 1 June 2009

* Supported by Major State Basic Research Development Program of China (2007CB815005), National Natural Science Foundation of China (10825522, 10735010, 10775158) and Chinese Academy of Sciences

1) E-mail: yhzhang@impcas.ac.cn

2 Experimental methods and results

High-spin states of the odd-proton nucleus ^{139}Pm were populated through the ^{116}Cd(^{27}Al, 4n)^{139}Pm reaction at a beam energy of 120 MeV. The ^{27}Al beam was provided by the HI-13 accelerator at the China Institute of Atomic Energy (CIAE), Beijing. The target consisted of 2.2 mg/cm^2 ^{116}Cd foil (94% enrichment) backed with a 7 mg/cm^2 evaporated lead layer. An array of thirteen Compton-suppressed Ge detectors was used to collect the in-beam γ rays. About 1.9×10^8 coincidence events were accumulated and sorted into a 4k×4k E_{γ_1}-E_{γ_2} matrix for subsequent analysis. Both ^{133}Ba and ^{152}Eu sources were used for the energy and efficiency calibration of the detectors.

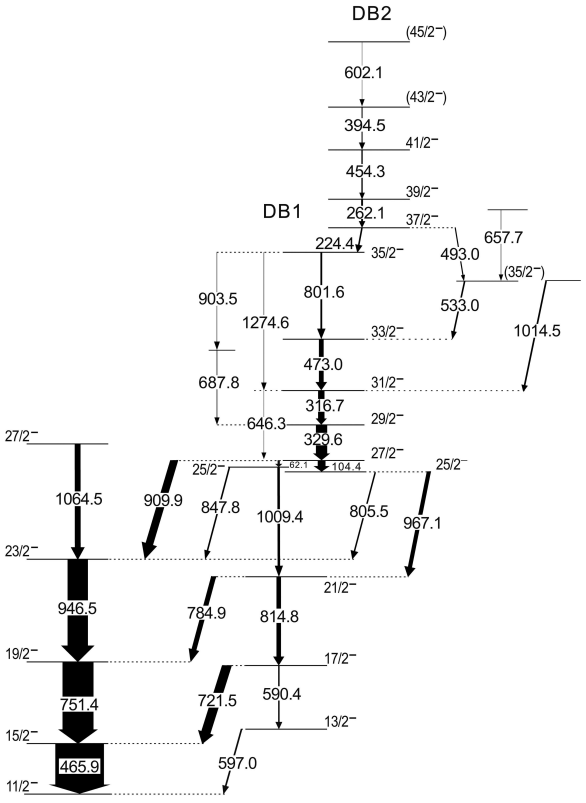

Fig. 1. Partial level scheme of ^{139}Pm.

The partial level scheme deduced from this work is shown in Fig. 1. It was constructed from the γ-γ coincidence relationships, the relative γ-transition intensities and the DCO ratio analysis. The results of our analysis such as the γ-transition energies, the relative transition intensities and the assignments of spin and parity (I^π) are presented in Table 1. The transition intensities have been normalized to that of the 751.4 keV γ-ray. The DCO ratios are obtained by gating on 465.9 keV E2 transition. It is clear from Table 1 that most of the transitions in the bands DB1 and DB2 have M1 nature as they lie around 0.5. The DCO ratios for 801.6, 454.3, 394.5 and 602.1 keV transitions could not be determined from a gate on 465.9 keV. Therefore, Table 1 shows the DCO ratios for a gate on 329.6 keV M1 transition, and the values range between 0.8 and 1.2 indicating the M1 character with a spin change of $\Delta I = 1$.

Table 1. γ-ray energies, relative intensities, spin and parity assignments, and DCO ratios in ^{139}Pm.

E_γ/keV[a]	I_γ[b]	assignment	DCO ratio[c]
		DB1	
329.6	36.4	$29/2^- \rightarrow 27/2^-$	0.61(3)
316.7	20.6	$31/2^- \rightarrow 29/2^-$	0.61(5) 0.97(13)*
473.0	15.3	$33/2^- \rightarrow 31/2^-$	0.47(4) 0.90(8)*
801.6	5.8	$35/2^- \rightarrow 33/2^-$	0.85(17)*
646.3	1.6	$31/2^- \rightarrow 27/2^-$	1.01(16)
687.8	3.0	$(31/2^-) \rightarrow 29/2^-$	0.97(20)*
903.5		$35/2^- \rightarrow (31/2^-)$	
1274.6	$\leqslant$1.7	$35/2^- \rightarrow 31/2^-$	
		DB2	
224.4	5.0	$37/2^- \rightarrow 35/2^-$	0.66(8) 1.12(16)*
262.1	6.0	$39/2^- \rightarrow 37/2^-$	0.55(12) 1.08(18)*
454.3	4.0	$41/2^- \rightarrow 39/2^-$	0.98(14)*
394.5	3.1	$(43/2^-) \rightarrow 41/2^-$	0.80(18)*
602.1	1.0	$(45/2^- \rightarrow 43/2^-)$	0.93(52)*
		other transitions	
62.1			
104.4			
465.9	156.6	$15/2^- \rightarrow 11/2^-$	
493.0	6.0	$37/2^- \rightarrow (35/2^-)$	0.98(30)*
533.0	5.0	$(35/2^-) \rightarrow 33/2^-$	0.62(14)
590.4	4.6	$17/2^- \rightarrow 13/2^-$	1.51(40)*
597.0	5.2	$13/2^- \rightarrow 11/2^-$	0.94(25)*
657.7	1.5		
721.5	$\leqslant$21.7	$17/2^- \rightarrow 15/2^-$	0.42(6)
751.4	100.0	$19/2^- \rightarrow 15/2^-$	0.93(3)
784.9	13.0	$21/2^- \rightarrow 19/2^-$	0.44(6)
805.5	3.3	$25/2^- \rightarrow 23/2^-$	0.44(14)
814.7	14.5	$21/2^- \rightarrow 17/2^-$	0.90(15)
847.8	4.0	$25/2^- \rightarrow 23/2^-$	0.97(20)*
909.9	22 .3	$27/2^- \rightarrow 23/2^-$	0.87(9)
946.5	65.7	$23/2^- \rightarrow 19/2^-$	0.93(2)
967.1	13.4	$25/2^- \rightarrow 21/2^-$	1.57(14)*
1009.4	8.0	$25/2^- \rightarrow 21/2^-$	0.89(8)
1014.5	5.1		0.56(8)
1064.5	18.8	$27/2^- \rightarrow 23/2^-$	0.96(6)

[a] Uncertainties between 0.1 and 0.5 keV.
[b] Uncertainties between 5% and 30%. Corrected for the efficiency of Ge detectors.
[c] The DCO ratios marked with asterisk obtained with gate on 329.6 keV transition.

Two dipole bands have been observed in ^{139}Pm in the present work. Some coincidence γ-ray spectra are shown in Figs. 2 and 3. Fig. 2(a) shows a spectrum obtained by gating on the 909.9 keV γ-transition. Most of the transitions above the $27/2^-$ level can be seen. Fig. 1 shows the presence of prominent M1 transitions up to the spin $33/2^-$ in agreement with the results reported by Xu et al [12]. We add one new cascade transition 801.6 keV at the upper end of the sequence in DB1 which is in coincidence with 329.6, 316.7, 473.0 keV gamma rays. Fig. 2(b) shows a coincidence spectrum by gating on the 224.4 keV γ-transition in DB2. One can also see the corresponding coincidence γ rays in DB1.

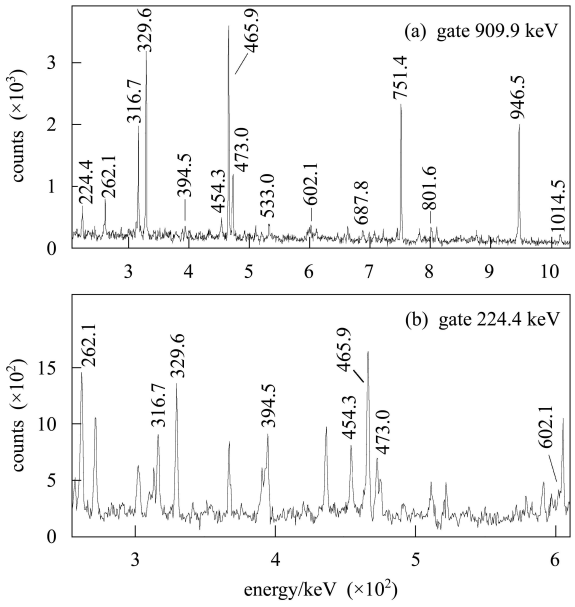

Fig. 2. Coincidence spectra of the dipole bands.

The ordering of the M1 transitions in DB1 has been further confirmed through the detection of crossover E2 transitions in DB1 for the first time. The crossover 646.3 keV ($31/2^- \rightarrow 27/2^-$) transition is shown in the (316.7 + 329.6 + 473.0) keV sum-gated spectrum in Fig. 3(a). The high energy 1274.6 keV crossover E2 transition is also shown in the sum spectrum in Fig. 3(b). The other linking transitions namely 493.0, 533.0, 687.8 keV are shown in Fig. 3(a). The new DB2 consists of five cascade transitions and no crossover transitions have been observed. It deexcites in a complex way into DB1 and the proposed spin assignments are based on its deexcitations and on the DCO ratios obtained for most of the in-band and connecting transitions.

Most of the levels and transitions reported in Ref. [12] were confirmed in the present work. At low spins, a strong 1009.4 keV E2 transition was observed, and two weak linking transitions of 805.5, 847.8 keV were added. Most of the gamma transitions below the $21/2^-$ level can be obviously seen when we gate on the 1009.4 keV γ-ray as shown in Fig. 3(c). But the 62.1 keV transition from $27/2^-$ to the $25/2^-$ level was not observed because of the lower detection efficiency for this energy. Taking into account the energy spacings of rotational cascades, 1009.4 keV E2 transition is possible to deexcite the unfavored signature member of the $h_{11/2}$ yrast band and the strong 967.1 keV transition deexites the bandhead of DB1.

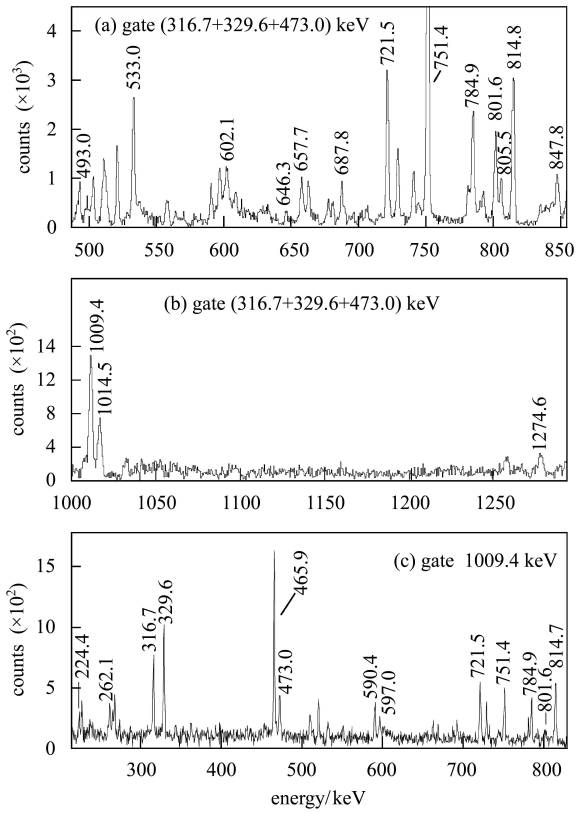

Fig. 3. (a) and (b) Sum spectra by gating on (316.7+329.6+473.0) keV. (c) Spectrum for a gate on 1009.4 keV.

3 Discussion

The most prominent feature of the level scheme shown in Fig. 1 is the presence of fairly strongly populated $\Delta I = 1$ sequences. Two regular dipole bands are observed and they show a small signature splitting. Crossover E2 transitions, which dominate in the normal bands, are very weak. In the N=78 nucleus ^{141}Eu, two dipole bands have been also found which were considered to be the MR bands on the basis of the lifetime measurement [10]. The level structure of ^{139}Pm is very similar to that of ^{141}Eu, that is, the spins of the DB1 in ^{139}Pm and ^{141}Eu are both measured from $25/2^-$ to $35/2^-$, and the DB2 from $35/2^-$

to $45/2^-$. Fig. 4 presents the plots of E-I and I-$\hbar\omega$ for the two dipole bands in both nuclei. Therefore it is natural to propose that the two dipole bands in ^{139}Pm may originate from the same mechanism. A configuration $\pi h_{11/2} \otimes \nu(h_{11/2})^{-2}$ may be assigned to DB1 and a $\pi h_{11/2} \otimes \nu(h_{11/2})^{-4}$ configuration to DB2. An analogous situation also exists in the neighboring nucleus ^{137}Pr [8], where a three-quasiparticle $\pi h_{11/2} \otimes \nu(h_{11/2})^{-2}$ configuration has been interpreted as MR band. The $\Delta I = 1$ level sequences built on the I=$25/2^-$ level in the odd-Z nuclei may have the same structure. The B(M1)/B(E2) ratios could be deduced for only one crossover transition of 646.3 keV and the value $35(\mu_N/\mathrm{eb})^2$ is typical for MR bands in this region. Previously these kinds of bands are interpreted as an oblate collective structure built on oblate neutron and proton states in a standard model. But attainable experimental B(M1) values show a sharp decrease with increasing angular momentum that can not be reproduced by the standard cranking model. An appropriate description of the observed properties of the Ml bands has been provided in the frame of the tilted axis cranking (TAC) model [3]. Most lifetime measurements give a clear support to the interpretation of the dipole bands in terms of the shears mechanism. The behavior of the B(M1) values is a definitive way to confirm the nature of the dipole bands and differentiate between TAC and standard cranking calculations. So lifetime measurements are needed to determine these bands's structure in ^{139}Pm.

The dipole bands in ^{139}Pm can be associated with a small oblate deformation of the nucleus due to the alignment of neutrons. For this shape the $h_{11/2}$ proton states with large Ω values and the $h_{11/2}$ neutron-hole states with small Ω values contribute to the configurations of the dipole bands. Considering an alignment of the spins of the particle states along the symmetry axis and of the hole states along the rotation axis, angular momenta of $25/2$ and $33/2\hbar$, respectively, are expected for the bandheads of DB1 and DB2. In the level scheme of Fig. 1 the dipole band DB1 starts with $I = 25/2$, indicating that the contribution from core collective rotation is almost absent which is one of the characteristics in MR bands. But DB2 starts with $I = 37/2$, about $2\hbar$ larger than the calculated value, suggesting that the deformation for DB2 is larger than for DB1 caused by the alignment of a second $\nu h_{11/2}$ hole pair.

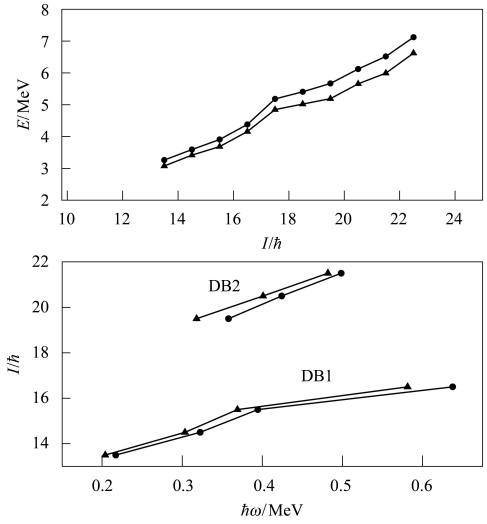

Fig. 4. A comparison of the measured energy E vs spin I and of the experimental spin I vs the rotational frequency $\hbar\omega$ for these two dipole bands in ^{139}Pm (solid circles) and ^{141}Eu (solid triangles).

In summary, the odd mass nucleus ^{139}Pm has been studied to high spins in order to investigate the magnetic rotation phenomenon in the mass 130 region. Two $\Delta I = 1$ bands have been observed. Strong M1 transitions with several weak crossover E2 transitions have been found suggesting their magnetic-rotational character. And the comparison between ^{139}Pm and ^{141}Eu nuclei also supports a magnetic rotation nature for both dipole bands. However, for a more detailed investigation of the features of these bands of ^{139}Pm, further experiments are required.

The authors are grateful to the staff of the in-beam γ-ray group and the tandem accelerator group at CIAE for their help during the experiment and for providing the heavy-ion beam and the target.

References

1 Frauendorf S. Nucl. Phys. A, 2000, **677**: 115
2 Hübel H. Prog. Part. Nucl. Phys., 2005, **54**: 1
3 Frauendorf S. Nucl. Phys. A, 1993, **557**: 259
4 Clark R M, Asztalos S J, Busse B et al. Phys. Rev. Lett., 1999, **82**: 3220
5 Jenkins D G, Wadsworth R, Cameron J A et al. Phys. Rev. Lett., 1999, **83**: 500
6 Chiara C J, Asztalos S J, Busse B et al. Phys. Rev. C, 2000, **61**: 034318.
7 Lakshmi S, Jain H C, Joshi P K et al. Phys. Rev. C, 2002, **66**: 041303(R)
8 Agarwal Priyanka, Kumar Suresh, Singh Sukhjeet et al. Phys. Rev. C, 2007, **76**: 024321
9 Brandolini F, Ionescu-Bujor M, Medina N H et al. Phys. Lett. B, 1996, **388**: 468
10 Podsvirova E O, Lieder R M, Pasternak A A et al. Eur. Phys. J. A, 2004, **21**: 1
11 Klinken J van, Feenstra S J. Phys. Rev. C, 1975, **12**: 2111
12 XU N, Beausang C W, Paul E S et al. Phys. Rev. C, 1987, **36**: 1649